Original Article

MOLECULAR METABOLISM

# Silver nanoparticles inhibit beige fat function and promote adiposity

Lishu Yue [1,4], Wenjun Zhao [1,4], Dongmei Wang [1,4], Meiyao Meng [1], Ying Zheng [1], Yu Li [1], Jin Qiu [1], Jian Yu [1], Yang Yan [1], Peng Lu [2], Youmin Sun [3], Jie Fu [3], Jiqiu Wang [2], Qiang Zhang [1], Lingyan Xu [1,**], Xinran Ma [1,*]

## ABSTRACT

**Objective:** Obesity is a complex chronic disease of high prevalence worldwide. Multiple factors play integral roles in obesity development, with rising interest focusing on the contribution of environmental pollutants frequent in modern society. Silver nanoparticles (AgNPs) are widely used for bactericidal purpose in various applications in daily life. However, their potential toxicity and contribution to the obesity epidemic are not clear.
**Methods:** Beige adipocytes are newly discovered adipocytes characterized by high thermogenic and energy dissipating capacity upon activation and the "browning" process. In the present study, we assess the impact of AgNPs exposure on beige adipocytes differentiation and functionality both *in vitro* and *in vivo*. We also systematically investigate the influence of AgNPs on adiposity and metabolic performance in mice, as well as the possible underlying molecular mechanism.
**Results:** The results showed that, independent of particle size, AgNPs inhibit the adipogenic, mitochondrial, and thermogenic gene programs of beige adipocytes, thus suppressing their differentiation ability, mitochondrial activity, and thermogenic response. Importantly, exposure to AgNPs in mice suppresses browning gene programs in subcutaneous fat, leading to decreased energy expenditure and increased adiposity in mice. Mechanistically, we found that AgNPs increase reactive oxidative species (ROS) levels and specifically activate MAPK-ERK signaling in beige adipocytes. The negative impacts of AgNPs on beige adipocytes can be ameliorated by antioxidant or ERK inhibitor FR180204 treatment.
**Conclusions:** Taken together, these results revealed an unexpected role of AgNPs in promoting adiposity through the inhibition of beige adipocyte differentiation and functionality, possibly by disrupting ROS homeostasis and ERK phosphorylation. Future assessments on the health risk of AgNPs applications and their safe dosages are warranted.


**Keywords** Adiposity; Beige fat; Silver nanoparticles; Browning; Energy expenditure; Reactive oxidative species

## 1. INTRODUCTION

Obesity, a chronic disease of multifactor and complex nature, is the major risk factor for metabolic diseases including diabetes, fatty liver, cardiovascular diseases, and certain types of cancer. The obesity epidemic seriously threatens public health and poses great economic burden to modern society [1]. Well-established factors contributing to obesity development include genetic susceptibility, excessive energy intake, and sedentary lifestyle with new clues continuing to emerge [2]. Notably, recent interest has focused on environmental pollutants for their wide impact on daily life and their close link to obesity and metabolic diseases [3].

In a triumph of modern industry technologies, numerous synthetic compounds are commercialized and offer great convenience to ordinary households and manufacturers alike. However, when released into the environment, some of these compounds or byproducts produced during their manufacturing processes pose significant threats to the ecosystem and human health [4]. For instance, it is well recognized that some chemicals have hormone-disrupting effects and contribute to the development of obesity and metabolic disorders [5], a few examples being organochlorine as a dry cleaning reagent or pesticide [6,7], bisphenol A (BPA) commonly used for plastic synthesis [8,9], and polybrominated diphenyl in many flame retardant products [10,11]. In addition, ambient air pollution, a problem faced by most large cities, has been reported to exaggerate insulin resistance and visceral inflammation/adiposity as demonstrated by mice model exposed to fine particulate matter PM2.5 [12].

Besides synthetic compounds and air particles, with the fast development of nanotechnology emerges another category of environmental pollutants: nanoparticles [13]. Nanoparticles, ultrafine particles of 1–100 nm in size, bring unique optical, electrical, or thermal properties to

[1]Shanghai Key Laboratory of Regulatory Biology, Institute of Biomedical Sciences and School of Life Sciences, East China Normal University, Shanghai, 200241, China [2]Department of Endocrinology and Metabolism, China National Research Center for Metabolic Diseases, Ruijin Hospital, Shanghai Jiao Tong University School of Medicine, Shanghai, 200025, China [3]Department of Environmental Science & Engineering, Fudan University, Shanghai, 200433, China

[4] These authors contributed equally to this work.

*Corresponding author. E-mail: xrma@bio.ecnu.edu.cn (X. Ma).

**Corresponding author. E-mail: lyxu@bio.ecnu.edu.cn (L. Xu).

Received October 13, 2018 • Revision received January 9, 2019 • Accepted January 19, 2019 • Available online 24 January 2019

https://doi.org/10.1016/j.molmet.2019.01.005

 

the products when used in corporation with bulk materials [14]. The recent decade has seen an exponential growth in the fabrication of nanoparticles, commonly termed as engineered nanoparticles (ENPs), due to their extensive use in engineering technologies and in consumer products [15]. Of the most widely used ENPs, silver nanoparticles (AgNPs) attract growing interest due to their extraordinary antibacterial, optical, and conductive properties, and have been widely applied in numerous aspects of life, including water refreshment systems, apparel, appliances, milk bottles, cosmetics, and plastics, as well as components of biosensors and optical equipment. The wide usage of AgNPs in daily life has raised concerns about their safety and potential influence on human health. For instance, AgNPs can release silver ions or produce reactive oxygen species (ROS), which may disrupt cell membrane structure, protein aggregation, mitochondria functionality, and metabolic homeostasis [16]. However, the potential contribution of AgNPs to the obesity epidemics as well as the underlying mechanism have not been addressed.

Obesity manifests as excessive fat accumulation and metabolic impairment in adipocytes. Three distinct classes of adipocytes exist that feature different anatomical, morphological, and functional properties [17]. White adipocytes store energy in the form of triglycerides while brown adipocytes, named after their brownish color due to high mitochondrial contents, are thermogenically poised upon activation and dissipate energy through uncoupling protein 1 (UCP1), enriched in mitochondria [18]. The newly discovered beige adipocytes intersperse in clusters within white adipose tissues and function similarly as brown adipocytes (thus termed "beige", white in brown). They are highly inducible and activated upon cold or β-agonists stimuli through the "browning" process to increase energy expenditure [19]. Of potential therapeutic significance, cold-inducible beige adipocytes exist in human adults, and their activation is significantly diminished in obese and aged populations [20,21]. Thus, beige adipocytes are considered important peripheral targets in combating obesity.

In the present study, we assess the impact of AgNPs exposure on obesity by studying the *in vitro* effects of AgNPs on beige adipocytes differentiation and functionality, as well as their *in vivo* influence on beige fat and metabolic parameters of mice under high fat diet. Our results demonstrated that AgNPs suppress beige adipocyte development and functionality via increased ROS-ERK signaling, resulting in increased adiposity in mice. Our study suggested that environmental exposure of AgNPs may contribute to the obesity epidemic, and scrutiny is warranted in the safe applications of silver nanoparticles in the future.

## 2. MATERIALS AND METHODS

### 2.1. Materials

Different sizes of AgNPs were purchased from Dk Nano technology. The AgNPs were dispersed by ultra-sonication in DMSO for *in vitro* studies or in mineral oil for animal studies of 5 mg/mL stocks and diluted to their final concentrations. All the AgNPs solutions were freshly prepared from stock solutions and ultrasonicated for 3 min before use.

### 2.2. Characterization of AgNPs

The transmission electron microscopy (TEM) images of AgNPs were obtained using a transmission electron microscope (Hitachi) operated at an accelerating voltage of 100 kV. The UV-Vis spectra of AgNPs were recorded using a Cary 60 UV-Vis spectrophotometer (Agilent Technologies). The hydrodynamic sizes of AgNPs were recorded with Zetasizer Nano ZS90 (Malvern).

### 2.3. Cell culture, primary adipocyte isolation and differentiation

C3H10T1/2 cells were obtained from ATCC and were maintained in Dulbecco's Modified Eagle Medium (DMEM) supplemented with 10% fetal bovine serum and 1% penicillin and streptomycin in a humidified incubator at 37 °C with 5% $CO_2$. Cells were maintained into a confluent state until differentiation. For differentiation procedure, confluent C3H10T1/2 cells were induced to differentiate to beige/brown adipocytes in differentiation medium supplemented with 5 μg/ml insulin, 0.5 mM 3-isobutyl-1-methylxanthine, 5 μM dexamethasone, 0.125 mM indomethacin, 50 nM T3, and 1 μM rosiglitazone for 48 h and subsequently cultured in maintenance medium supplemented with 5 μg/ml insulin, 50 nM T3 and 1 μM rosiglitazone. The maintenance medium was changed every 2 days. The cells were collected on the 7th day.

Primary adipocyte isolation and differentiation was performed as previously described [22]. Briefly, mice epididymal fat, subcutaneous fat, and brown fat were isolated, finely minced, and subjected to collagenase digestion. The stromal vascular fraction (SVF) was pelleted and resuspended in DMEM medium containing 25 mM glucose, 20% FBS, 20 mM Hepes, 1% penicillin, and streptomycin, and culture medium was changed daily. For brown and beige adipocyte differentiation assays, the isolated SVFs from iWAT and BAT were stimulated with culture medium containing 10% FBS, penicillin and streptomycin supplemented with 0.5 mM 3-isobutyl-1-methylxanthine, 125 μM indomethacin, 1 μM dexamethasone, 6 μg/ml insulin, 50 nM T3, and 1 μM rosiglitazone, for 48 h and subsequently cultured in maintenance medium (6 μg/ml insulin, 50 nM T3 and 1 μM rosiglitazone) for another 6 days. For white adipocyte differentiation, SVFs from eWAT were stimulated with culture medium containing 10% FBS, penicillin and streptomycin supplemented with 6 μg/ml insulin, 0.5 mM 3-isobutyl-1-methylxanthine, 10 μM dexamethasone and 10 μg troglitazone for 48 h and maintained in 6 μg/ml insulin for another 6 days. N-Acetyl-L-cysteine (NAC) and FR180204 were purchased from Sigma and treated in cells as indicated.

### 2.4. Cellular metabolic rates

Cellular metabolic rates were measured using a XF24 Analyzer (Seahorse Bioscience). Primary beige adipocytes were differentiated for 6 days and treated with or without Ag20NPs for 24 h. Respiration was measured under basal conditions and with the complex III inhibitor antimycin A. We calculated basal oxygen consumption rate (OCR) as the value resulting from the difference between basal OCR and OCR measured after antimycin A addition and normalized to the quantity of protein levels.

### 2.5. MTT assay

Cell viability was evaluated using the MTT Cell Proliferation and Cytotoxicity assay kit (Sigma). Briefly, C3H10T1/2 cells were seeded into 96-well culture plate at a density of about $1 \times 10^4$ cells/well and 100 μl DMEM medium containing 10% FBS was added to each well. 10 μl of MTT solution (5 mg/ml) were added to each well and incubated for 4 h at 37 °C. Subsequently, the medium was removed and 100 μL of formazan dissolving solution was added to each well and cells were incubated at 37 °C until formazan was totally dissolved into the solution. Finally, the optical density (OD) value of each well at 570 nm was measured and recorded using SpectraMax 190 Microplate Reader (Molecular Devices).

### 2.6. RNA extraction and quantitative PCR

Total RNA was extracted from cultured cells with RNAiso Plus (TaKaRa), and 1 μg total RNA was reverse transcribed to cDNA using

 

the PrimeScriptTM RT Master Mix (TaKaRa). Quantitative Real-time PCR was performed using the HieffTM qPCR SYBR® Green Master Mix (Low Rox Plus) (Yeasen) on the QuantStudio3 (Thermo Fisher Scientific). qPCR was then conducted under the following conditions: 95 °C for 5 min, 40 cycles at 95 °C for 10 s, 60 °C for 20 s and 72 °C for 20 s, 95 °C for 15 s, 60 °C for 1 min and 95 °C for 15 s. Experiments were repeated three times. The data were normalized to 36B4 levels and relative mRNA expression levels were calculated using the $2^{-\Delta\Delta CT}$ method. Sequences of primers used for real-time PCR are listed in Table S1.

### 2.7. Lipid staining and oil red O quantitative analysis

Cells were fixed with 10% paraformaldehyde for 15 min at room temperature. After fixation, cells were washed once with PBS and 60% isopropyl alcohol then stained with a filtered ORO (Sigma) working solution for 20 min at room temperature. After the cells were photographed, the ORO was eluted with 60% isopropyl alcohol for 10 min at room temperature. The optical density (OD) value of each well at 520 nm was measured and recorded using SpectraMax 190 Microplate Reader.

### 2.8. Fluorescence and flow-cytometry analysis with mitotracker

Mitochondria quality and membrane integrity were assessed by staining with MitoTracker® Red CMXRos (Thermo Fisher). After treatment with 5 μg/ml of AgNPs for 24 h, mature C3H10T1/2 adipocytes were incubated with 100 nM of Mitotracker for 15 min and then washed three times with PBS. Fluorescent images were obtained using the Nikon inverted microscope ECLIPSE Ts2. Cells were then digested by 0.25% trypsin and redissolved in PBS. After cells were filtered, mean fluorescent intensity of adipocytes was detected using BD LSRFortessaTM flow cytometer, and data were analyzed using FlowJo software.

### 2.9. Detection of intracellular ROS

Intracellular ROS levels were measured by the DCF assay. In brief, differentiated C3H10T1/2 adipocytes ($5 \times 10^3$cells/well) were seeded in black 96-well plates. Differentiated C3H10T1/2 adipocytes with different treatment were incubated with 50 μM DCFH-DA (Sigma) and then washed three times with DMEM. After the cells were photographed, mean DCF fluorescent intensities were detected using a SpectraMax M2 microplate fluorometer (Molecular Devices).

### 2.10. Western blot analysis

Cells were harvested and washed once with cold PBS. Proteins were extracted with RIPA buffer consisting 50 mM Tris (pH7.4), 150 mM NaCl, 1% NP-40, 0.25% sodium deoxycholate, 1 mM PMSF, 10 mM DTT and protease inhibitors. The protein lysates were collected using a scraper and separated by 10% sodium dodecyl sulfonate-polyacrylamide gel electrophoresis (SDS-PAGE) and then transferred into a NC membrane (PALL, 66485). After blocking with 5% skimmed milk, the membrane was incubated overnight at 4 °C with primary antibodies, including anti-UCP1 (Abcam, ab10983), anti-PGC1α (Santa Biotechnology, sc-517380) and anti-β-actin (Santa Biotechnology, sc-47778), antibodies against MAPKs were purchased from Cell Signaling Technology including p-p38 (4511S), p38α (2371S), p-JNK(4671S), JNK(9252S), p-ERK (9106S) and ERK (4695S). Subsequently, the membrane was incubated with secondary antibodies at room temperature, including Goat anti-Mouse (LI-COR, 926-68070) and Goat anti-Rabbit (LI-COR, 926-68071). The images of western blots were collected and analyzed by Odyssey® CLx Imaging System (LI-COR).

### 2.11. TEM analysis of cells

Differentiated C3H10T1/2 adipocytes were treated with vehicle or 5 μg/ml AgNPs for 24 h, digested by 0.25% trypsin and then fixed by 2.5% glutaraldehyde for TEM imaging. TEM images were obtained with Hitachi 7650 TEM operating at 80 kV and a digital camera from Advanced Microscopy Techniques.

### 2.12. Animal studies

Mouse studies were performed according to the guidelines of the East China Normal University Animal Care and Use Committee. C57BL/6J mice were purchased from Shanghai Research Center for Model Organisms and kept at a humidity environment with free access to food and water and in a standard light-dark cycle. In acute treatment, 2-month-old male mice ($n = 4$ per group) were intragastrically administrated 125 mg/kg AgNPs or injected with 5 mg/kg AgNPs into bilateral inguinal fat pads and silver ion concentration or gene expression analysis were performed 48 h after treatment. In chronic treatment for metabolic assessment, mice under high fat diet (60%, ResearchDiet) were injected with 5 mg/kg AgNPs in inguinal fat pads bilaterally once a month for three times ($n = 6$ per group). Body weights and body compositions were measured once a week using Meg-Med MRI system. Energy expenditure measurements were performed at the end of treatment. Briefly, mice were housed individually and oxygen consumption was recorded at room temperature using a 12-chamber CLAMS system (Columbus Instruments) after at least 48 h of adaptation period. Total locomotor activity was determined by infrared beam interruption (Opto-Varimex mini, Columbus Instruments), and food intake was measured during indirect calorimetry measurement. Mice were then sacrificed one month after last injection for tissue analysis.

### 2.13. Lipid and liver function assays

Total cholesterol, HDL-C, triglyceride (TG), alanine amino transferase (ALT), and aspartate amino transferase (AST) levels in serum were detected according to the manufacturer's instructions (Jiancheng, Nanjing, China). TG in liver samples was extracted using 5% NP-40, with samples heated at 90 °C for twice. The transparent supernatant was collected and measured using the commercial kits (Jiancheng, Nanjing, China).

### 2.14. Histological evaluation and immunohistochemistry (IHC) analysis

Adipose or liver tissues were fixed in 10% buffered formalin. Hematoxylin and eosin staining was performed on paraffin-embedded sections (5 μm thick). UCP1 immunostaining procedure was according to our previous report [22], UCP1 primary antibody (Ab10983, Abcam) and Anti-rabbit HRP-conjugated secondary antibody (D110058, Sangon) were incubated. Then 3,3′-diaminobenzidine tetrahydrochloride (HRP-DAB) followed by nuclear staining with hematoxylin was performed.

### 2.15. Measurement of tissue silver ion concentrations

Tissues were digested with 10 mL nitric acid and 1 mL 30% hydrogen peroxide and heated at 150 °C until the fluid was boiled. After cooling, 2 mL perchloric acid was added and heated again at 150 °C till the fluid was less than 1 mL and then diluted by adding $ddH_2O$ to the volume of 50 mL. The concentration of silver ion was analyzed using an atomic absorption spectrophotometer (contrAA300, Analytik Jena).

### 2.16. Statistical analysis

A student's t-test was used to compare two groups. One-way ANOVA followed by the Dunnett post hoc test was used for multiple

 

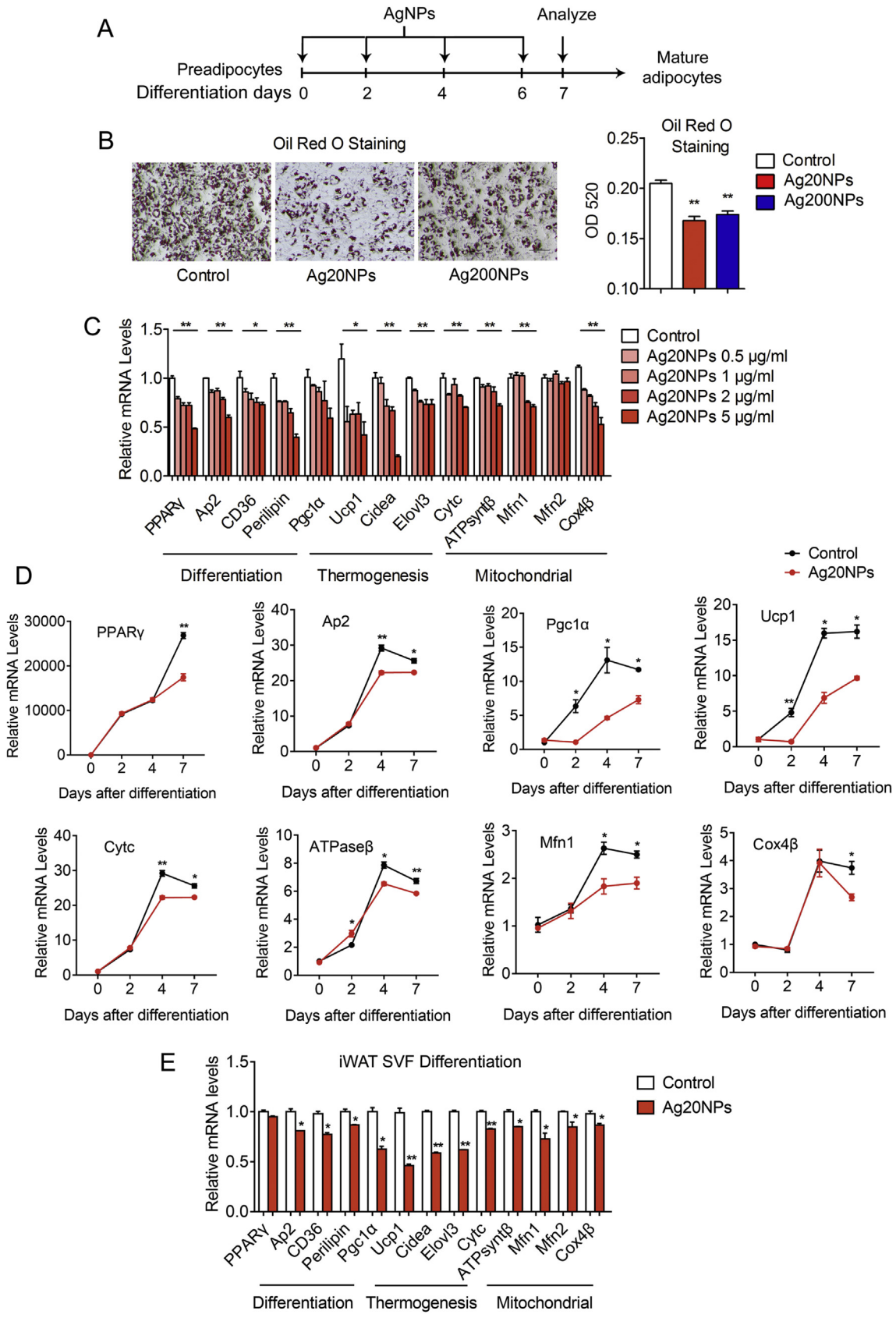


**Figure 1: AgNPs blocked differentiation of beige adipocytes.** (A) Experimental schematics of AgNP administration along the differentiation process of adipocytes. On the last day of differentiation, cells were harvested and analyzed. (B) Representative images of Oil red O staining (left) and quantification (right) in C3H10T1/2 adipocytes. (C–E) Quantitative PCR analysis of the influence of Ag20NPs on the differentiation and thermogenic and mitochondrial gene programs in C3H10T1/2 adipocytes (C) under different Ag20NPs doses or (D) on different days of differentiation, or (E) in primary beige adipocytes. Data are presented as mean ± SEM and *P < 0.05, **P < 0.01 compared to control group.

 

comparisons versus the control group (GraphPad Software). $P < 0.05$ was set as the criterion for statistical significance.

## 3. RESULTS

### 3.1. Characteristics of AgNPs

To recapitulate the influence of AgNPs on adiposity, instead of laboratory level AgNPs, we obtained engineered AgNPs commonly used in industrial applications for analyses. It is reported that the toxic effects of nanoparticles vary depending on their sizes. Thus, AgNPs of two sizes were examined in the present study. As shown in Figures S1A and S1B, TEM images revealed that these AgNPs were typically spherical or ellipsoidal with a relatively uniform size of $18.41 \pm 6.55$ nm and $185 \pm 23.85$ nm, respectively. Their hydrodynamic sizes were 21.0 nm (referred as Ag20NPs) and 220.2 nm (referred as Ag200NPs), respectively (Figures S1C), which were a bit larger than the size measured from TEM images. The UV-visible spectra showed that both Ag20NPs and Ag200NPs had a continuous absorption at 400–1000 nm (Figure S1D). Compared to laboratory level AgNPs, these engineered AgNPs for industry purposes show forms of aggregation, possibly due to different synthetic processes.

### 3.2. AgNPs suppress beige adipocyte differentiation and functionality

Two *in vitro* models were adopted to assess the influence of Ag20NPs and Ag200NPs on beige adipocytes: differentiated C3H10T1/2 adipocytes, a classic *in vitro* cellular model of beige adipocytes; and cultured primary beige adipocytes isolated from mouse subcutaneous fat (iWAT).

We first administered AgNPs in the process of adipocyte differentiation to assess their influences on beige adipocyte differentiation (Figure 1A). Ag20NPs or Ag200NPs (referred to as AgNPs below) of different doses were used as determined by MTT analysis that showed no impact on cell viability (Figure S2). Results indicated that, independent of particle size, AgNPs treatment significantly suppressed adipogenic capacity of beige adipocytes, as shown by Oil Red O staining (Figure 1B) and quantitative PCR examining adipogenic gene programs (Figure 1C, D, S3A and S3B). Expectedly, the presence of AgNPs also inhibited the thermogenic and mitochondrial gene programs in a dose- and time-dependent manner in both C3H10T1/2 adipocytes and primary beige adipocytes, possibly due to a lack of functional mature beige adipocytes (Figure 1C–E, S3A, S3B). Interestingly, AgNPs showed similar effects on primary white adipocytes but not on primary brown adipocytes (Figure S3C and S3D).

Next, we treated fully differentiated adipocytes with AgNPs to test their impacts on beige adipocyte functionality (Figure 2A). Cellular oxygen consumption rate analysis revealed that, independent of particle size, AgNP treatment inhibited basic oxygen consumption of primary beige adipocytes (Figure 2B). Consistently, AgNP exposure to beige adipocytes led to reduced thermogenic and mitochondrial gene programs in a dose-dependent manner (Figures 2C and S4A). Moreover, treatment of forskolin, a well-established cAMP agonist, caused a robust induction in thermogenic and mitochondrial gene programs in beige adipocytes, which was blocked by concomitant treatment with AgNPs (Figure 2D), especially in expression levels of PGC1$\alpha$ and UCP1 (Figure 2E), two master regulators in the browning process. These AgNP effects were recapitulated in primary beige adipocytes but were absent in primary brown adipocytes (Figures 2F and S4B). Overall, these data suggest that AgNPs interfere with beige adipocyte differentiation and functionality.

### 3.3. AgNP exposure inhibits energy expenditure and leads to increased adiposity in mice

Since *in vitro* data showed that, independent of particle sizes, AgNP treatment negatively impacted beige adipocytes differentiation and functionality, we then set out to unravel the *in vivo* effects of AgNP exposure using Ag20NP as a representative. As oral ingestion is among the major means of AgNP exposure to human body in daily life, we tested the acute effects of Ag20NPs in mice via intragastric administration using a previously reported safe dose [23]. Interestingly, we found that adipose tissues were sensitive to AgNP exposure, since the concentration of silver ions in iWAT, epididymal adipose tissues (eWAT), and brown fat (BAT) was comparable to that in liver, an organ reported to be predisposed to AgNP deposition via oral ingestion (Figure S5A). Furthermore, gene expression analysis revealed intragastric administration of AgNPs suppressed thermogenic and mitochondrial gene programs in iWAT (Figure S5B). Since oral administration of AgNP in mice caused significant silver ion penetration into all three kinds of adipose tissues, in order to focus on studying its influences on beige fat functionality *in vivo*, we directly injected Ag20NPs into mouse iWAT. This rendered similar silver ion concentrations in iWAT compared to intragastric administration, while at the same time largely reduced silver ion deposition in other metabolically active tissues, such as eWAT, BAT, liver, and gastrocnemius muscle (Figure S5C). Detailed analysis showed that, similar to oral administration, single exposure of Ag20NPs to mouse iWAT suppressed thermogenic and mitochondrial genes expression, while no apparent toxicity was observed, as shown by the low serum ALT and AST levels (Figures S5C–S5E). Thus, we chose this model for subsequent *in vivo* study to elucidate the impacts of chronic AgNP administration on beige adipocyte functions.

Compared to control group, multiple Ag20NPs exposure mitigated energy expenditure in mice as demonstrated by significantly diminished expression of brown gene programs (Figure 3A) and decreased UCP1 IHC staining (Figure 3B) in iWAT and, of physiological significance, reduced whole-body oxygen and carbon dioxide consumption (Figure 3C,D). Interestingly, the alteration in gene expressions by Ag20NP treatment was specific to iWAT, with minor effects to eWAT and no apparent change in BAT (Figures S5F and S5G), suggesting the importance and potential of beige adipocytes in the contribution of energy expenditure. Meanwhile, it has to be noted that locomotor activity and food intake were similar between two groups (Figure S5H), indicating the lack of toxicity of chronic Ag20NP treatment in mice.

Though comparable in body weight (Figure 4A), mice with multiple Ag20NP exposure accreted more fat mass and less lean mass compared to controls under high fat diet (HFD) (Figures 4B and S6A), accompanied by increased adipose tissue weight (Figure 4C), enlarged adipocyte size (Figure 4D), disrupted serum lipid profile (Figure 4E) and increased inflammatory genes in eWAT (Figure S6B). The Ag20NP treated groups of mice also showed increased extent of liver steatosis under HFD (Figure 4F,G), although with similar liver weights as controls (Figure S6C). Intriguingly, despite their overall comparable performances in the glucose and insulin tolerance tests (Figures S6D and S6E), further analysis revealed that Ag20NPs-treated mice featured higher serum glucose elevation 15 min after challenge (Figure 4H), supporting a potential role of Ag20NPs in predisposing mice to insulin resistance. Taken together, these data suggested that *in vivo* Ag20NPs exposure recapitulated the *in vitro* effects on beige adipocytes in both acute and long-term treated mice models, thus contributing to decreased energy expenditure and increased adiposity under high fat diet.

 

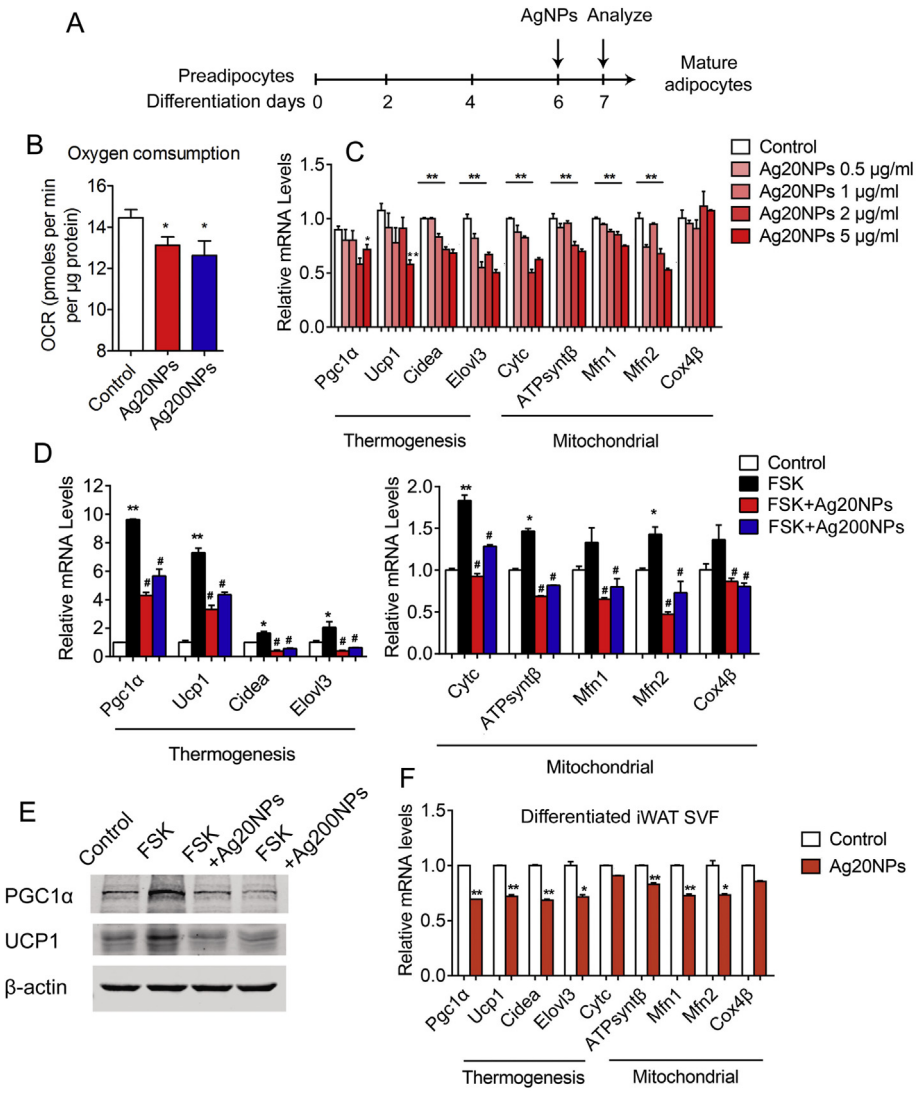


**Figure 2: AgNPs disrupted mitochondrial and thermogenic functions of beige adipocytes**. (A) Experimental schematics of AgNP administration on differentiated adipocytes. (B) Basal oxygen consumption in primary beige adipocytes. (C) Thermogenic and mitochondrial gene programs in C3H10T1/2 adipocytes under different Ag20NP doses. (D) AgNPs blocked forskolin (FSK)-induced elevation in the thermogenic (left) and mitochondrial (right) gene programs in C3H10T1/2 adipocytes. (E) AgNPs blocked forskolin (FSK)-induced elevation in PGC1α and UCP1 protein levels. (F) Ag20NP treatment inhibited thermogenic and mitochondrial gene programs in primary beige adipocytes. Data are presented as mean ± SEM and *P < 0.05, **P < 0.01 compared to control group. #P < 0.05 compared to FSK group.

### 3.4. AgNPs disrupt mitochondrial function via ROS-ERK signaling

As shown above, we observed consistent suppression of the thermogenic and mitochondrial gene programs in both iWAT and cultured beige adipocytes upon AgNP exposure. Next, we sought to offer mechanistic insights for the metabolic impacts of AgNPs. When stained with MitoTracker Red CMXRos, an indicator of mitochondrial integrity, AgNP-treated adipocytes showed weaker fluorescence signals in both microscopy examination and flow cytometry examination (Figure 5A,B), indicating loss of mitochondria membrane potential and impaired mitochondria function after AgNP exposure. Further examination with TEM revealed that AgNPs penetrated into adipocyte cytoplasm and resided mainly in endosomes and lysosomes (Figure S7), as previously reported [24,25]. It is known that AgNPs exert their cytotoxic effects mainly through releasing damaging silver ions in the acidic environment in endosomes and lysosomes, inducing reactive oxygen species (ROS) and elevating cellular redox stress, which interferes with many physiological processes, i.e. disrupts normal mitochondrial functions [25–27]. Indeed, we found elevated ROS levels and diminished thermogenic and mitochondrial gene programs in adipocytes after AgNP treatment, both were corrected by antioxidant NAC administration (Figure 5C,D). The MAPK signaling transduces cellular stresses, i.e. oxidative stress or disruption in ROS homeostasis, to downstream target gene modulations, thus governing physiological or pathological stress responses, including the regulation of energy expenditure [28]. We thus examined whether AgNPs impact beige adipocyte function through the MAPK pathways, which include ERK, p38 and JNK pathways. As shown in Figure 5E, Ag20NPs treatment specifically activated ERK phosphorylation, which was abrogated by NAC administration, while JNK or p38 remained unaffected. Furthermore, ERK inhibitor FR180204 treatment on adipocytes significantly reversed the AgNPs-mediated suppression on thermogenic and mitochondrial gene programs (Figure 5F). Taken together, these data suggested that AgNPs disrupt mitochondrial function at least partially by increasing ROS levels and activating ERK pathway, thus inhibiting

 

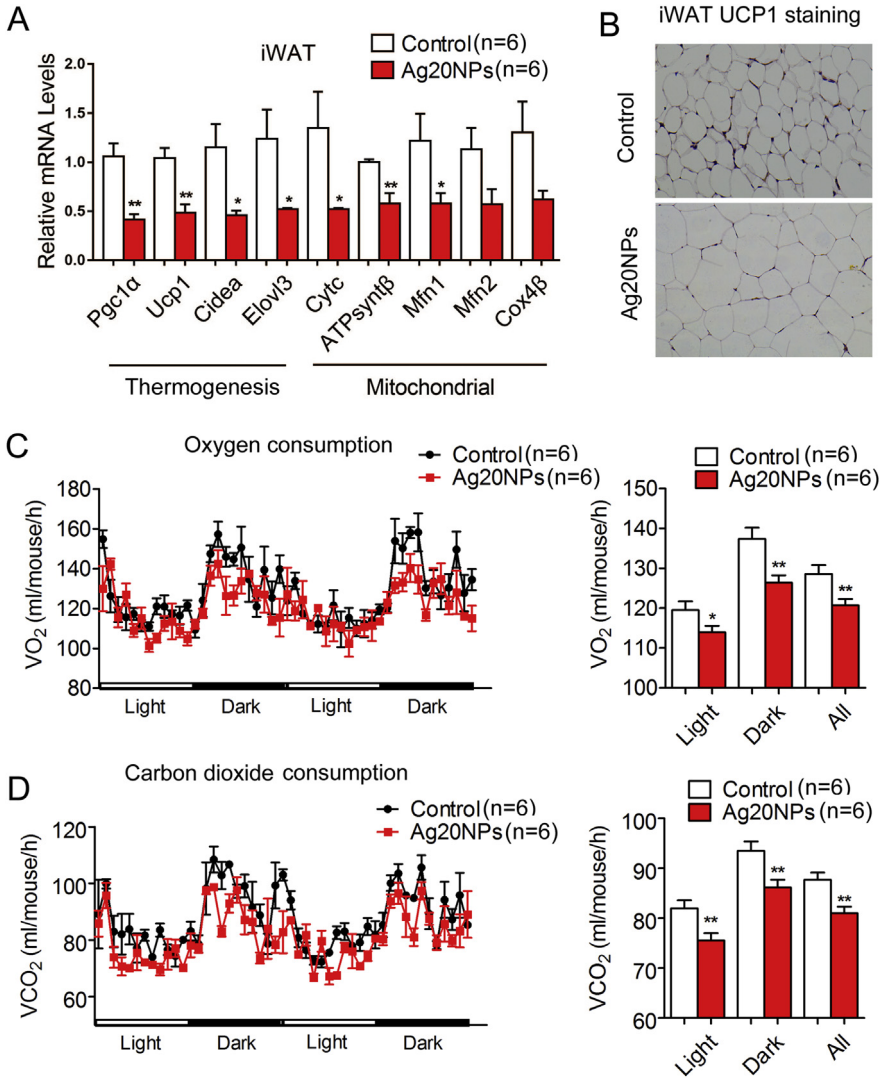


**Figure 3: AgNPs suppressed brown gene programs in subcutaneous fat and whole body energy expenditure in mice**. Mice under chronic treatment were treated with Ag20NPs or vehicle once a month for three months and sacrificed one month after last injection. (A) The thermogenic and mitochondrial gene programs in subcutaneous fat (iWAT). (B) Representative images of UCP1 immunostaining in iWAT. (C and D) Mice were analyzed in CLAMS for (C) oxygen consumption or (D) carbon dioxide consumption. n = 6 per group. Data are presented as mean ± SEM and *P < 0.05, **P < 0.01 compared to control group.

beige adipocyte functionality and, in turn, impacting whole-body energy balance (Figure 6).

## 4. DISCUSSION

The applications of silver nanoparticles (AgNPs) infiltrate every aspect of our daily life. They are commonly used in water treatment and in the manufacture of a wide range of items including house appliances, cosmetics, textiles, surgical instruments, etc. for their superior bactericidal property. While enjoying the convenience these advances bring it is vital to clearly assess the potential impacts of AgNPs on human health. In recent decades, obesity has risen as a severe global public health problem. The question of whether the prevalent use of nanoparticle products contributes to the obesity epidemic piqued our interest. To answer this question, we obtained the engineered AgNPs that are routinely used in industrial manufacturing and examined their influence on adiposity. Remarkably, we found that AgNPs significantly inhibited the adipogenic, thermogenic, and mitochondrial functions of beige adipocytes, a unique kind of adipocyte that is critical in energy dissipation. Moreover, in a diet-induced-obese mouse model, AgNP exposure to subcutaneous fat, a fat depot rich in beige adipocytes, led to metabolic impairments including suppressed energy expenditure, increased fat mass, and abnormal lipid/glucose homeostasis. These results indicated a potential role of AgNPs in obesity development, and cautions should be taken in future AgNP applications.

A growing body of evidences has linked obesity with various environmental pollutants, including dust, PM2.5, black carbon and BPA. Yet, how nanoparticles, substances with pleiotropic implications and thus frequent and constant contacts to human bodies, influence adiposity remain elusive. It is of note that previous reports focused on white fat and usually used white adipocyte cellular models to study the impacts of pollutants on obesity by promoting white adipocyte differentiation and lipogenesis governed by the master adipogenic regulator PPARγ [29,30]. However, recent research indicated that, instead of white adipocytes, the proper differentiation and functionality of energy consuming adipocytes, including brown and beige adipocytes, are the

 

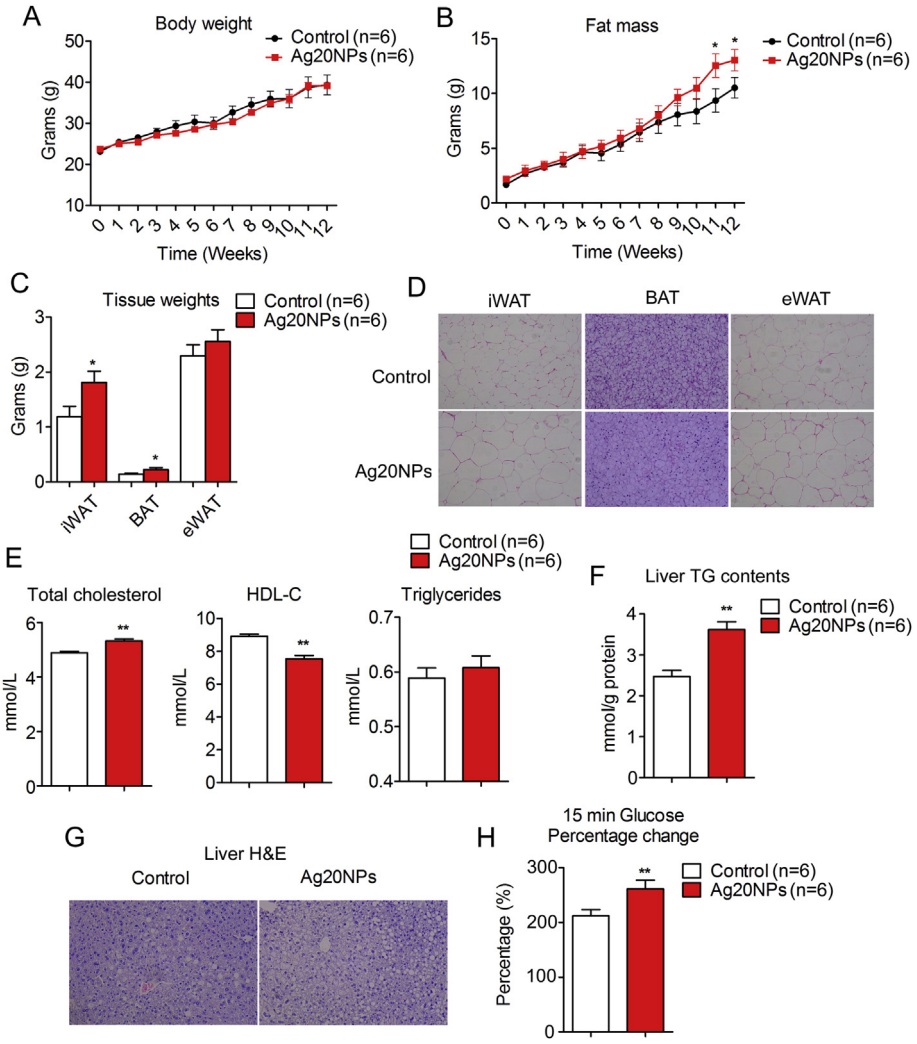


**Figure 4: AgNP exposure led to increased adiposity in mice**. Mice under chronic treatment were treated with Ag20NPs or vehicle once a month for three months and sacrificed one month after last injection. (A) Body weights; (B) Fat mass; (C) Weight of subcutaneous fat (iWAT), brown fat (BAT) and epididymal white fat (eWAT); (D) Representative images of H&E staining of adipocytes from iWAT, BAT and eWAT; (E) Serum levels of total cholesterol, HDL-C, triglycerides; (F) Liver TG contents; (G) Representative images of liver H&E staining and (H) percentage change of glucose induction after 15 min glucose challenge in glucose tolerance test. n = 6 per group. Data are presented as mean ± SEM and *P < 0.05, **P < 0.01 compared to control group.

driving forces behind energy imbalance and obesity [31]. With both *in vitro* and *in vivo* data, our present work demonstrated that AgNP exposure suppressed the thermogenic and mitochondrial gene programs of beige adipocytes, thus impairing beige fat activation (the "browning" process) and energy dissipation. These results strongly suggested that AgNPs, and potentially other environmental pollutants, may contribute to the obesity epidemic via disruption on energy homeostasis.

Kim et al. reported that 13-week oral administration with low-dose AgNPs (125 mg/kg) in rats showed no apparent toxicity, but changes in detailed metabolic parameters were not assessed [23]. In order to assess the *in vivo* influence of AgNPs on energy metabolism in a direct and specific manner, we injected AgNPs into subcutaneous fat, a method shown to be effective in modulating gene expression in specific fat depots to affect whole-body energy expenditures [21,22,32]. Furthermore, a very low dose of 5 mg/kg AgNPs was used in our study; although this concentration was much lower than the safe dose used in the study by Kim et al., it resulted in similar silver ion accumulation and gene expression changes in iWAT compared to intragastric administration models, while minimizing the side effects caused by silver ion penetration in other metabolic active tissues. Consistent with Kim et al., we found that mice exposed to 5 mg/kg AgNPs once a month over a 12-week timespan showed no apparent toxic effects and have similar body weights compared to control mice. However, importantly, detailed analysis revealed that AgNP delivery increased fat mass, suppressed energy expenditure, and disrupted serum lipid parameters in treated mice. Of note, our results demonstrated that AgNP exposure, even at a low concentration that caused no tissue toxicity, was sufficient to cause prolonged impairment of beige adipocyte function and disruption of energy homeostasis. Thus, a narrowing down of AgNP safety ranges may be warranted to take into consideration their impact on obesity and metabolic fitness.

Concomitant with increased fat mass, we also observed a decrease in lean mass in AgNPs-treated mice, possibly due to the influence of AgNPs on muscle or a potential fat-muscle crosstalk [33]. It would be necessary to systematically evaluate AgNPs' effects on various metabolic organs. Besides, under our current AgNP treatment regimen, we found a marginal yet significant change in glucose tolerance in

 

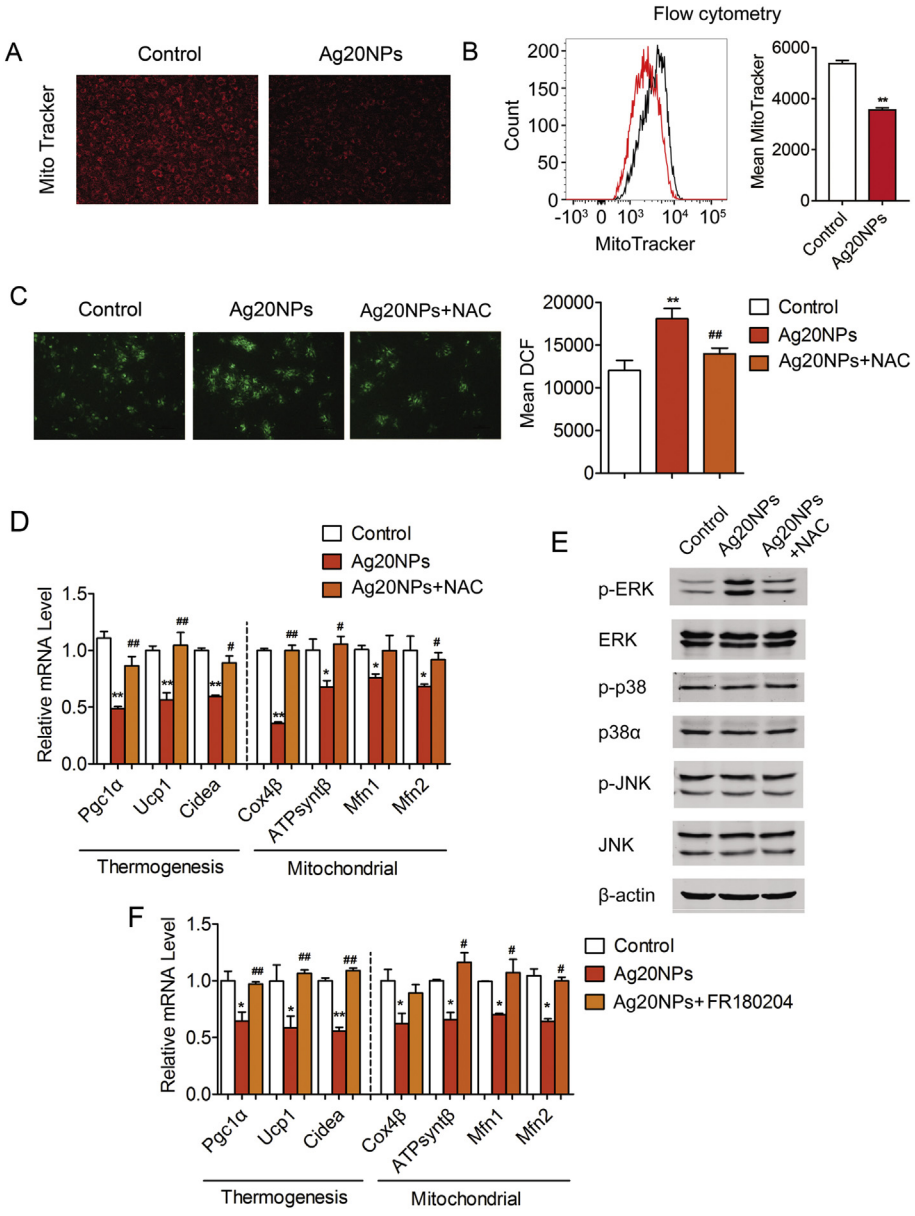


**Figure 5: AgNPs-ROS-ERK signaling mediates AgNP impact on adiposity**. (A) Representative fluorescent images of Mitotracker staining on differentiated C3H10T1/2 adipocytes treated with or without Ag20NPs. (B) Intensity of Mitotracker fluorescent signals was assessed by flow cytometry. (C and D) Differentiated C3H10T1/2 adipocytes were treated with vehicle, Ag20NPs or Ag20NPs plus antioxidant NAC. The reactive oxygen species (ROS) production in cells were assessed by DCF assay. Representative fluorescent images and quantification were shown in (C) and changes in brown gene programs were shown in (D). (E) Western blot assessing the phosphorylated and total MAPK signaling pathways of differentiated C3H10T1/2 adipocytes treated with vehicle, Ag20NPs or Ag20NPs plus NAC. (F) Differentiated C3H10T1/2 adipocytes were treated with vehicle, Ag20NPs or Ag20NPs plus specific ERK inhibitor FR180204 and changes in brown gene programs were assessed. Data are presented as mean ± SEM and *P < 0.05, **P < 0.01 compared to control group. #P < 0.05, ##P < 0.01 compared to Ag20NPs group.

treated mice. Future studies with increased treatment length or times are needed to assess the impact of AgNPs on insulin sensitivity.

Mechanistically, we found that AgNPs exert their deleterious effects on beige adipocytes by increasing ROS levels and in turn activating the ERK signaling pathway, which is reversible upon antioxidant NAC or ERK inhibitor FR180204 treatment. The disruption in ROS homeostasis has been shown to among the main mechanisms through which nanoparticles pose toxicity to various physiological processes including white adipocytes functionality [29,34]. Since various NAC supplement products are readily available on markets, it is possible to use NAC as a daily supplement to counteract the nanoparticle-induced toxicity in human. However, precautions must be taken in choosing a proper NAC dosage, as a finely balanced ROS homeostasis is critical in a plethora of physiological events, for example, the maintenance of thermogenic capacity of beige fat [35] and the regulation of cancer progression [36,37]. On the other hand, it has been shown that multiple nanoparticles stimulate MAPK signaling, especially via ERK and/or p38 phosphorylation to promote or inhibit physiological processes, including adipocyte and osteoblast differentiation [29,38]. ERK signaling has been previously reported to suppress thermogenesis and energy expenditure in adipocytes by inhibiting UCP1 or activating inflammatory signaling [39]. Moreover, genetic and pharmacological

 

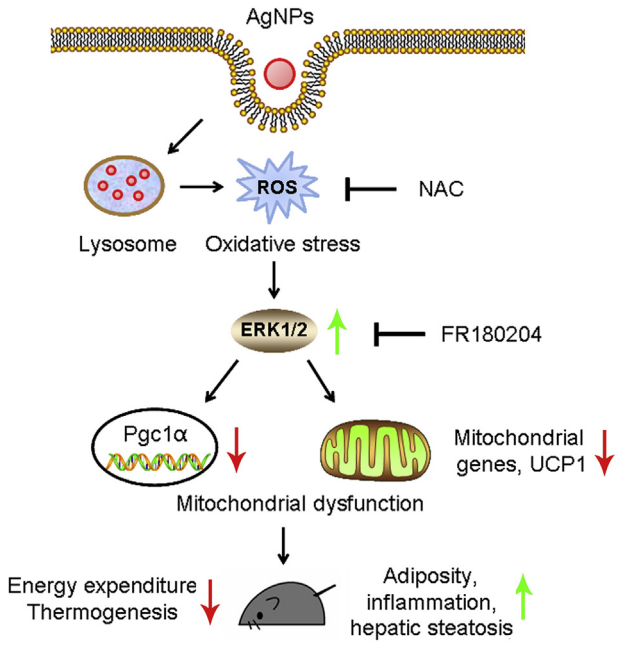


**Figure 6: Impact of AgNPs on beige adipocytes and mouse physiology**. After AgNPs exposure, nanoparticles enter the cytoplasm and reside in lysosomes, releasing ROS into the lysosomal acidic environment. The elevated, cellular ROS levels cause oxidative stress and increase ERK phosphorylation, which, in turn, suppress thermogenic and mitochondrial gene programs including PGC1α and UCP1. AgNPs exposure caused mitochondrial dysfunction leads to decreased energy expenditure and increased adiposity in mice.

interventions on p38 phosphorylation have been shown to suppress browning of white fat via PKA-CREB pathways [40], suggesting that the activation of MAPK signaling pathways has a negative impact on energy homeostasis. In our study, we found that the adverse cellular effects caused by AgNP treatment in beige adipocytes, i.e. elevated ROS levels and suppressed thermogenic and mitochondrial gene programs are corrected by NAC or FR180204 administration. It would be worthwhile to systematically evaluate the effects of NAC or MAPK inhibitors on cellular and animal models exposed to AgNPs, for example, mitochondrial integrity, respiration rate and whole body fat content, to assess their potential involvement in combating the metabolic challenges brought by nanoparticles. It would also be interesting to investigate the selective activation of different MAPK pathways by different nanoparticles.

In conclusion, our results demonstrated that low dose AgNP exposure disrupts energy homeostasis and promotes adiposity, emphasizing the importance of restricting AgNP environmental release and exposure to humans in the future. Mechanistically, our data demonstrated that the development and functionality of beige adipocytes are impacted by AgNPs via increased ROS-ERK signaling pathway, suggesting that NAC supplement at proper dosages or treatment with ERK inhibitors may be beneficial to combat the contribution of nanoparticles on the current obesity epidemics.

## ACKNOWLEDGEMENTS

This project is supported by funds from the National Natural Science Foundation of China (31770840 to X.M and 31800989 to L.X), Shanghai Pujiang Program (17PJ1402600 to X.M and 17PJ1402700 to L.X), the Program for Professor of Special Appointment (Eastern Scholar) at Shanghai Institutions of Higher Learning (TP2017042 to X.M) and China Postdoctoral Science Foundation (2017M611499 to D.W and 2018M632068 to W.Z). The authors have declared no conflict of interest.

## CONFLICT OF INTEREST

None declared.

## APPENDIX A. SUPPLEMENTARY DATA

Supplementary data to this article can be found online at https://doi.org/10.1016/j.molmet.2019.01.005.

## REFERENCES

[1] Friedrich, M.J., 2017. Global obesity epidemic worsening. Journal of the American Medical Association 318(7):603. https://doi.org/10.1001/jama.2017.10693.

[2] Yazdi, F.T., Clee, S.M., Meyre, D., 2015. Obesity genetics in mouse and human: back and forth, and back again. Peer J 3:e856. https://doi.org/10.7717/peerj.856. eCollection 2015.

[3] Dangi-Garimella, S., 2014. Environmental pollutants: a risk factor for obesity and diabetes. American Journal of Managed Care 20(10 Spec No):E8.

[4] Lee, D.H., Porta, M., Jacobs Jr., D.R., Vandenberg, L.N., 2014. Chlorinated persistent organic pollutants, obesity, and type 2 diabetes. Endocrine Reviews 35(4):557–601. https://doi.org/10.1210/er.2013-1084.

[5] Karoutsou, E., Polymeris, A., 2012. Environmental endocrine disruptors and obesity. Endocrine Regulations 46(1):37–46.

[6] Tang, M., Chen, K., Yang, F., Liu, W., 2014. Exposure to organochlorine pollutants and type 2 diabetes: a systematic review and meta-analysis. PLoS One 9(10):e85556. https://doi.org/10.1371/journal.pone.0085556.

[7] Rosenbaum, P.F., Weinstock, R.S., Silverstone, A.E., Sjödin, A., Pavuk, M., 2017. Metabolic syndrome is associated with exposure to organochlorine pesticides in Anniston, AL, United States. Environment International 108:11–21. https://doi.org/10.1016/j.envint.2017.07.017.

[8] Wang, T., Li, M., Chen, B., Xu, M., Xu, Y., Huang, Y., et al., 2012. Urinary bisphenol A (BPA) concentration associates with obesity and insulin resistance. The Journal of Clinical Endocrinology and Metabolism 97(2):E223–E227. https://doi.org/10.1210/jc.2011-1989.

[9] Hao, M., Ding, L., Xuan, L., Wang, T., Li, M., Zhao, Z., et al., 2018. Urinary bisphenol A concentration and risk of central obesity in Chinese adults: a prospective study. Journal of Diabetes 10(6):442–448. https://doi.org/10.1111/1753-0407.12531.

[10] Erkin-Cakmak, A., Harley, K.G., Chevrier, J., Bradman, A., Kogut, K., Huen, K., et al., 2015. In utero and childhood polybrominated diphenyl ether exposures and body mass at age 7 years: the CHAMACOS study. Environmental Health Perspectives 123(6):636–642. https://doi.org/10.1289/ehp.1408417.

[11] Vuong, A.M., Braun, J.M., Sjödin, A., Webster, G.M., Yolton, K., Lanphear, B.P., et al., 2016. Prenatal polybrominated diphenyl ether exposure and body mass index in children up to 8 Years of age. Environmental Health Perspectives 124(12):1891–1897. https://doi.org/10.1289/EHP139.

[12] Sun, Q., Yue, P., Deiuliis, J.A., Lumeng, C.N., Kampfrath, T., Mikolaj, M.B., et al., 2009. Ambient air pollution exaggerates adipose inflammation and insulin resistance in a mouse model of diet-induced obesity. Circulation 119(4):538–546. https://doi.org/10.1161/CIRCULATIONAHA.108.799015.

[13] Batista, C.A., Larson, R.G., Kotov, N.A., 2015. Nonadditivity of nanoparticle interactions. Science 350(6257):1242477. https://doi.org/10.1126/science.1242477.

[14] Toor, F., Miller, J.B., Davidson, L.M., Nichols, L., Duan, W., Jura, M.P., et al., 2016. Nanostructured silicon via metal assisted catalyzed etch (MACE):

 

chemistry fundamentals and pattern engineering. Nanotechnology 27(41): 412003. https://doi.org/10.1088/0957-4484/27/41/412003.

[15] Sharma, V.K., Filip, J., Zboril, R., Varma, R.S., 2015. Natural inorganic nanoparticles - formation, fate, and toxicity in the environment. Chemical Society Reviews 44(23):8410–8423. https://doi.org/10.1039/c5cs00236b.

[16] Bartłomiejczyk, T., Lankoff, A., Kruszewski, M., Szumiel, I., 2013. Silver nanoparticles - allies or adversaries? Annals of Agricultural and Environmental Medicine 20(1):48–54.

[17] Farmer, S.R., 2008. Molecular determinants of brown adipocyte formation and function. Genes and Development 22(10):1269–1275. https://doi.org/10.1101/gad.1681308.

[18] Nedergaard, J., Cannon, B., 2014. The browning of white adipose tissue: some burning issues. Cell Metabolism 20(3):396–407. https://doi.org/10.1016/j.cmet.2014.07.005.

[19] Long, J.Z., Svensson, K.J., Tsai, L., Zeng, X., Roh, H.C., Kong, X., et al., 2014. A smooth muscle-like origin for beige adipocytes. Cell Metabolism 19(5):810–820. https://doi.org/10.1016/j.cmet.2014.03.025.

[20] Olivier, B., Farmer, S.R., 2012. Recruitment of brown adipose tissue as a therapy for obesity-associated diseases. Frontiers in Endocrinology (Lausanne) 3:14. https://doi.org/10.3389/fendo.2012.00014.

[21] Ma, X., Xu, L., Gavrilova, O., Mueller, E., 2014. Role of forkhead box protein A3 in age-associated metabolic decline. Proceedings of the National Academy of Sciences of the United States of America 111(39):14289–14294. https://doi.org/10.1073/pnas.1407640111.

[22] Ma, X., Xu, L., Alberobello, A.T., Gavrilova, O., Bagattin, A., Skarulis, M., et al., 2015. Celastrol protects against obesity and metabolic dysfunction through activation of a HSF1-PGC1α transcriptional Axis. Cell Metabolism 22(4):695–708. https://doi.org/10.1016/j.cmet.2015.08.005.

[23] Kim, Y.S., Song, M.Y., Park, J.D., Song, K.S., Ryu, H.R., Chung, Y.H., et al., 2010. Subchronic oral toxicity of silver nanoparticles. Particle and Fibre Toxicology 7:20. https://doi.org/10.1186/1743-8977-7-20.

[24] Chen, J., Guo, Z., Wang, H.B., Zhou, J.J., Zhang, W.J., Chen, Q.W., 2014. Multifunctional mesoporous nanoparticles as pH-responsive Fe(2+) reservoirs and artemisinin vehicles for synergistic inhibition of tumor growth. Biomaterials 35(24):6498–6507. https://doi.org/10.1016/j.biomaterials.2014.04.028.

[25] Guo, D., Zhao, Y., Zhang, Y., Wang, Q., Huang, Z., Ding, Q., et al., 2014. The cellular uptake and cytotoxic effect of silver nanoparticles on chronic myeloid leukemia cells. Journal of Biomedical Nanotechnology 10(4): 669–678.

[26] Chairuangkitti, P., Lawanprasert, S., Roytrakul, S., Aueviriyavit, S., Phummiratch, D., Kulthong, K., et al., 2013. Silver nanoparticles induce toxicity in A549 cells via ROS-dependent and ROS-independent pathways. Toxicology in Vitro 27(1):330–338. https://doi.org/10.1016/j.tiv.2012.08.021.

[27] Sun, C., Yin, N., Wen, R., Liu, W., Jia, Y., Hu, L., et al., 2016. Silver nanoparticles induced neurotoxicity through oxidative stress in rat cerebral astrocytes is distinct from the effects of silver ions. Neurotoxicology 52:210–221. https://doi.org/10.1016/j.neuro.2015.09.007.

[28] Son, Y., Kim, S., Chung, H.T., Pae, H.O., 2013. Reactive oxygen species in the activation of MAP kinases. Methods in Enzymology 528:27–48. https://doi.org/10.1016/B978-0-12-405881-1.00002-1.

[29] Son, M.J., Kim, W.K., Kwak, M., Oh, K.J., Chang, W.S., Min, J.K., et al., 2015. Silica nanoparticles inhibit brown adipocyte differentiation via regulation of p38 phosphorylation. Nanotechnology 26(43):435101. https://doi.org/10.1088/0957-4484/26/43/435101.

[30] Kassotis, C.D., Hoffman, K., Stapleton, H.M., 2017. Characterization of adipogenic activity of house dust extracts and semi-volatile indoor contaminants in 3t3-L1 cells. Environmental Science and Technology 51(15):8735–8745. https://doi.org/10.1021/acs.est.7b01788.

[31] Rosen, E.D., Spiegelman, B.M., 2014. What we talk about when we talk about fat. Cell 156(1–2):20–44. https://doi.org/10.1016/j.cell.2013.12.012.

[32] Xu, L., Ma, X., Verma, N.K., Wang, D., Gavrilova, O., Proia, R.L., et al., 2018. Ablation of PPARγ in subcutaneous fat exacerbates age-associated obesity and metabolic decline. Aging Cell 17(2):e12721. https://doi.org/10.1111/acel.12721.

[33] Boström, P., Wu, J., Jedrychowski, M.P., Korde, A., Ye, L., Lo, J.C., et al., 2012. A PGC1-α-dependent myokine that drives brown-fat-like development of white fat and thermogenesis. Nature 481(7382):463–468. https://doi.org/10.1038/nature10777.

[34] Rocca, A., Mattoli, V., Mazzolai, B., Ciofani, G., 2014. Cerium oxide nanoparticles inhibit adipogenesis in rat mesenchymal stem cells: potential therapeutic implications. Pharmaceutical Research 31(11):2952–2962. https://doi.org/10.1007/s11095-014-1390-7.

[35] Chouchani, E.T., Kazak, L., Jedrychowski, M.P., Lu, G.Z., Erickson, B.K., Szpyt, J., et al., 2016. Mitochondrial ROS regulate thermogenic energy expenditure and sulfenylation of UCP1. Nature 532(7597):112–116. https://doi.org/10.1038/nature17399.

[36] Sayin, V.I., Ibrahim, M.X., Larsson, E., Nilsson, J.A., Lindahl, P., Bergo, M.O., 2014. Antioxidants accelerate lung cancer progression in mice. Science Translational Medicine 6(221):221ra15. https://doi.org/10.1126/scitranslmed.3007653.

[37] Le, G.K., Ibrahim, M.X., Wiel, C., Sayin, V.I., Akula, M.K., Karlsson, C., et al., 2015. Antioxidants can increase melanoma metastasis in mice. Science Translational Medicine 7(308):308re8. https://doi.org/10.1126/scitranslmed.aad3740.

[38] Qin, H., Zhu, C., An, Z., Jiang, Y., Zhao, Y., Wang, J., et al., 2014. Silver nanoparticles promote osteogenic differentiation of human urine-derived stem cells at noncytotoxic concentrations. International Journal of Nanomedicine 9: 2469–2478. https://doi.org/10.2147/IJN.S59753.

[39] Sakamoto, T., Takahashi, N., Sawaragi, Y., Naknukool, S., Yu, R., Goto, T., et al., 2013. Inflammation induced by RAW macrophages suppresses UCP1 mRNA induction via ERK activation in 10T1/2 adipocytes. American Journal of Physiology Cell Physiology 304(8):C729–C738. https://doi.org/10.1152/ajpcell.00312.2012.

[40] Zhang, S., Cao, H., Li, Y., Jing, Y., Liu, S., Ye, C., et al., 2018. Metabolic benefits of inhibition of p38α in white adipose tissue in obesity. PLoS Biology 16(5):e2004225. https://doi.org/10.1371/journal.pbio.2004225.

 